Electronic Supplementary Material (ESI) for ChemComm.

Supporting information

Electronic Structure Inspired Highly Robust Electrocatalyst for Oxygen Evolution Reaction

Peng Zhang[a,§], Ying-Rui Lu[b,§], Chia-Shuo Hsu[c,§], Huai-Guo Xue[a], Ting-Shan Chan[b], Nian-Tzu Suen[a,], and Hao Ming Chen[b,c,*]*

[a]College of Chemistry & Chemical Engineering, Yangzhou University, Yangzhou 225002 (China)

[b]National Synchrotron Radiation Research Center, Hsinchu 300 (Taiwan)

[c]Department of Chemistry, National Taiwan University, Taipei 106 (Taiwan)

[*]Corresponding author: Nian-Tzu Suen (006641@yzu.edu.cn) and Hao Ming Chen (haomingchen@ntu.edu.tw)

Experimental Section

Materials and samples preparation. Nickel powder (99.5 %), red phosphorus (99.999 % metals basis) and KOH (ACS grade) were all purchased from Aladdin. In the process of synthesis, nickel and phosphorus were first weighted based on the stoichiometric ratio of the nominal chemical formula (Ni_5P_4, Ni_5P_2 and Ni_3P, total mass around 1 g) and then mixed evenly by grinding the materials for 10 mins. The mixed powder was then pressed into a pellet and sealed in a vacuum quartz tube. The tubes were placed in Muffle furnace and heated to 850 ℃ (with a ramping rate of 200 ℃/ h). After annealing for four days, the products were allowed to cool to room temperature by turning off the power of furnace. The tubes were then transferred into an Argon-filled glovebox in case that the product is air-sensitive. Carefully breaking the quartz tube and grinding the pellet into powder with agate pestle and mortar, the final product was stored in glovebox for further characterization and electrochemical measurement.

Characterization and Electrochemical Measurement. The morphology and composition of as-synthesized materials was studied by using scanning electron microscopy (SEM, Zeiss, model: Supra 55) and energy dispersive X-ray spectroscopy technique (EDS). Acceleration voltage was set to 30 keV that enabled us to detect corresponding elements. The crystal structure and purity of as-synthesized materials was analyzed with using Bruker D8 ADVANCE powder X-ray diffractometer (PXRD, Cu $K_{\alpha 1}$ radiation, $\lambda = 1.54056$ Å). The range of 2 θ was fixed from 25 ° to 60 ° with a step size of 0.05 °.

To examine the intrinsic electrocatalytic performance of title compounds, the as-synthesized materials were pressed into pellets (~ 100 mg) without any additives (e.g. binders or conductive materials). All electrochemical characterizations were investigated by using CHI-660E (CHI-potentiostat) with a standard three-electrode configuration cell (Hg/HgO as reference electrode; carbon rod as counter electrode). Typical electrochemical experiments were carried out in an electrolyte of 1.0 M KOH solution (pH = 14, ~ 40 ml) and the electrolyte has been purified (6 hrs electrolysis) to eliminate the Fe impurity. All potentials were adjusted with respect to reversible hydrogen electrode (RHE) including 90% of ohmic potential drop losses (R_u).

$E_{RHE} = E_{ref} + 0.05916*pH-i*R_u$

Notice that if the phase transformation occurred during oxygen evolution reaction (*i.e.* covert to metal oxyhydroxide), it usually accompanied with dissolving part of electrocatalyst in

electrolyte (anions like P, S, or Se). Accordingly, inductively coupled plasma mass spectrometry (ICP-MS, PerkinElmer, model: Elan DRC-e) was used to monitor Ni and P concentration (ppb) change in electrolyte every two hours through chronoamperometry test.

Theoretical calculation. The unit cell parameters and atomic positions for Ni_5P_4, Ni_5P_2 and Ni_3P were all been optimized by using ASE and GPAW software[1-3] before electronic structure calculation. The deviation between experiment reported and calculation optimized values of each cell length is less than 1 %. The model for Ni_5P_4 and Ni_3P is relatively straightforward since there is no disorder in their reported crystal structures. However, the case in Ni_5P_2 is slightly complicated because one Ni atom in the asymmetric unit would split into two (50 % on each) due to the bonding environment and results in a non-meaningful theoretical band structure (short Ni–Ni bond length, < 1 Å). To resolve this issue, we lower the space group from $P6_3cm$ to $P6_3$ that allows us to create two individual Ni atoms on this site. Therefore, one can eliminate either Ni atom and obtains an "ordered" form of Ni_5P_2 model for further band structure calculation.

To interrogate the electronic band structures and the chemical bonding interactions of Ni_5P_4, Ni_5P_2 and Ni_3P, their total and partial density of states (TDOS and PDOS), and crystal orbital Hamiltonian populations (COHP) of selected atomic interactions were computed with Stuttgart TB-LMTO 4.7 program.[4-6] The local density approximation (LDA) was used to treat exchange and correlation. The symmetry of the potential was considered spherical inside each Wigner–Seitz (WS) sphere,[7] and a combined correction was used to take into account the overlapping part. The radii of WS spheres were determined by an automatic procedure and were as follows: Ni = 1.29–1.48 Å and P = 1.34–1.56 Å. The basis sets included 4s, 4p and 3d for Ni; 3s, 3p, and 3d orbitals for P. The k-space integrations were made using the tetrahedron method, and irreducible k-points were set above at least one hundred in the Brillouin zone for all three case. We have to note here that the title compounds were tested and showed non-magnetic behaviors at room temperature. Nevertheless, we still performed spin-polarized calculations and there is no noticeable difference between spin-polarized and non-polarized calculations.

Reference

1. Mortensen, J. J.; Hansen, L. B.; Jacobsen, K. W., *Phys. Rev. B* **2005,** *71* (3), 035109.
2. Hjorth Larsen, A.; Jørgen Mortensen, J.; Blomqvist, J.; Castelli, I. E.; Christensen, R.; Dułak, M.; Friis, J.; Groves, M. N.; Hammer, B.; Hargus, C.; Hermes, E. D.; Jennings, P. C.; Bjerre Jensen, P.; Kermode, J.; Kitchin, J. R.; Leonhard Kolsbjerg, E.; Kubal, J.; Kaasbjerg, K.; Lysgaard, S.; Bergmann Maronsson, J.; Maxson, T.; Olsen, T.; Pastewka, L.; Peterson, A.; Rostgaard, C.; Schiøtz, J.; Schütt, O.; Strange, M.; Thygesen, K. S.; Vegge, T.; Vilhelmsen, L.; Walter, M.; Zeng, Z.; Jacobsen, K. W., *J. Phys. Condens. Matter* **2017,** *29* (27), 273002.
3. Enkovaara, J.; Rostgaard, C.; Mortensen, J. J.; Chen, J.; Dułak, M.; Ferrighi, L.; Gavnholt, J.; Glinsvad, C.; Haikola, V.; Hansen, H. A.; Kristoffersen, H. H.; Kuisma, M.; Larsen, A. H.; Lehtovaara, L.; Ljungberg, M.; Lopez-Acevedo, O.; Moses, P. G.; Ojanen, J.; Olsen, T.; Petzold, V.; Romero, N. A.; Stausholm-Møller, J.; Strange, M.; Tritsaris, G. A.; Vanin, M.; Walter, M.; Hammer, B.; Häkkinen, H.; Madsen, G. K. H.; Nieminen, R. M.; Nørskov, J. K.; Puska, M.; Rantala, T. T.; Schiøtz, J.; Thygesen, K. S.; Jacobsen, K. W., *J. Phys. Condens. Matter* **2010,** *22* (25), 253202.
4. Dronskowski, R.; Bloechl, P. E., *J. Phys. Chem.* **1993,** *97* (33), 8617−8624.
5. Jepsen, O.; Andersen, O. K. TB-LMTO-ASAP program, version 4.7, Max-Planck-Institut für Festkörperforschung, Stuttgart, Germany, 1998.
6. Barth, U. v.; Hedin, L., *J. Phys. C: Solid State Phys.* **1972,** *5* (13), 1629−1642.
7. Andersen, O. K., *Phys. Rev. B* **1975,** *12* (8), 3060−3083.

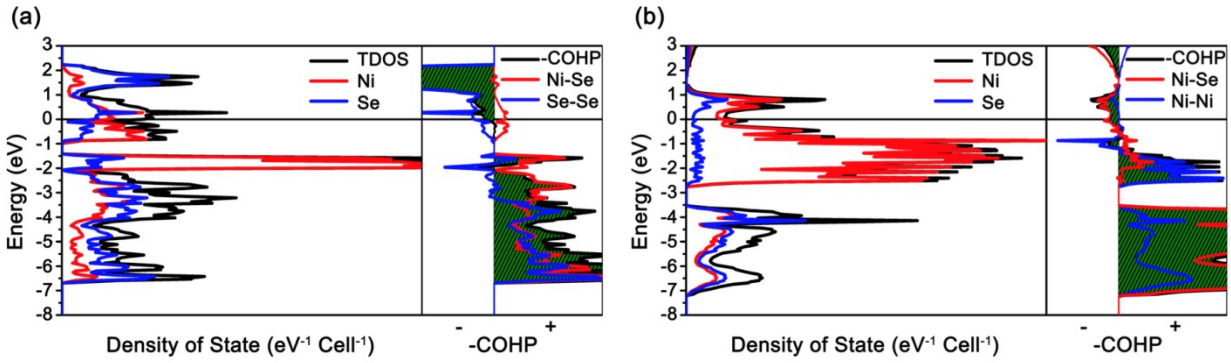

Figure S1. Calculated TDOS, PDOS curves for (a) $NiSe_2$ (b) Ni_3Se_2 along with the COHP curves for the Ni−Se, Ni−Ni and Se−Se interactions. In the −COHP curves, the positive and negative signs represent bonding and antibonding states, respectively.

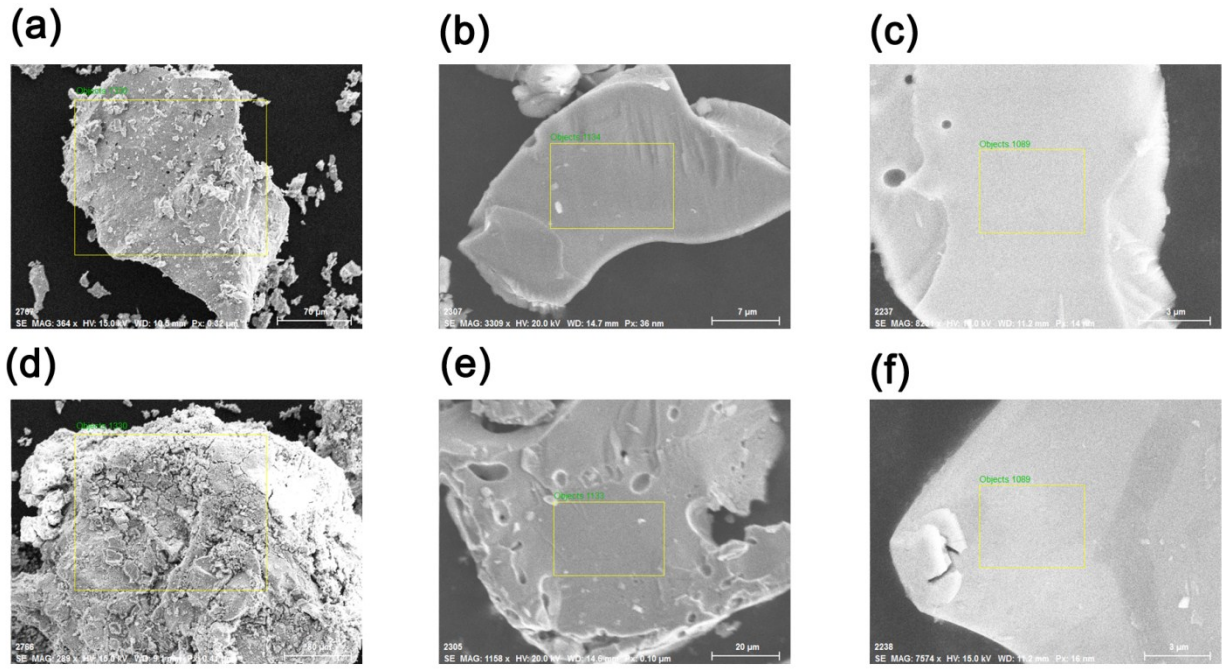

Figure S2. SEM images of Ni_5P_4 (a,d), Ni_5P_2 (b,e) and Ni_3P (c,f) before (top row) and after (bottom row) chronoamperometry test. The yellow box in the image is the selected area for EDS analysis and the result is shown in **Figure S3**.

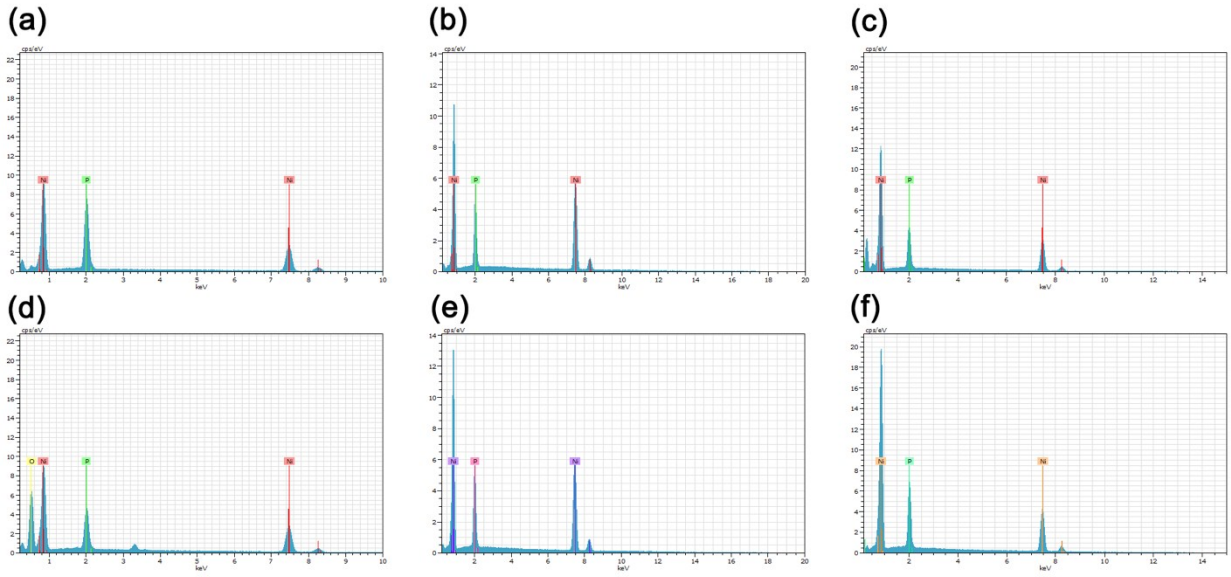

Figure S3. EDS of Ni_5P_4 (a, d), Ni_5P_2 (b, e) and Ni_3P (c, f) before (top row) and after (down row) chronoamperometry test.

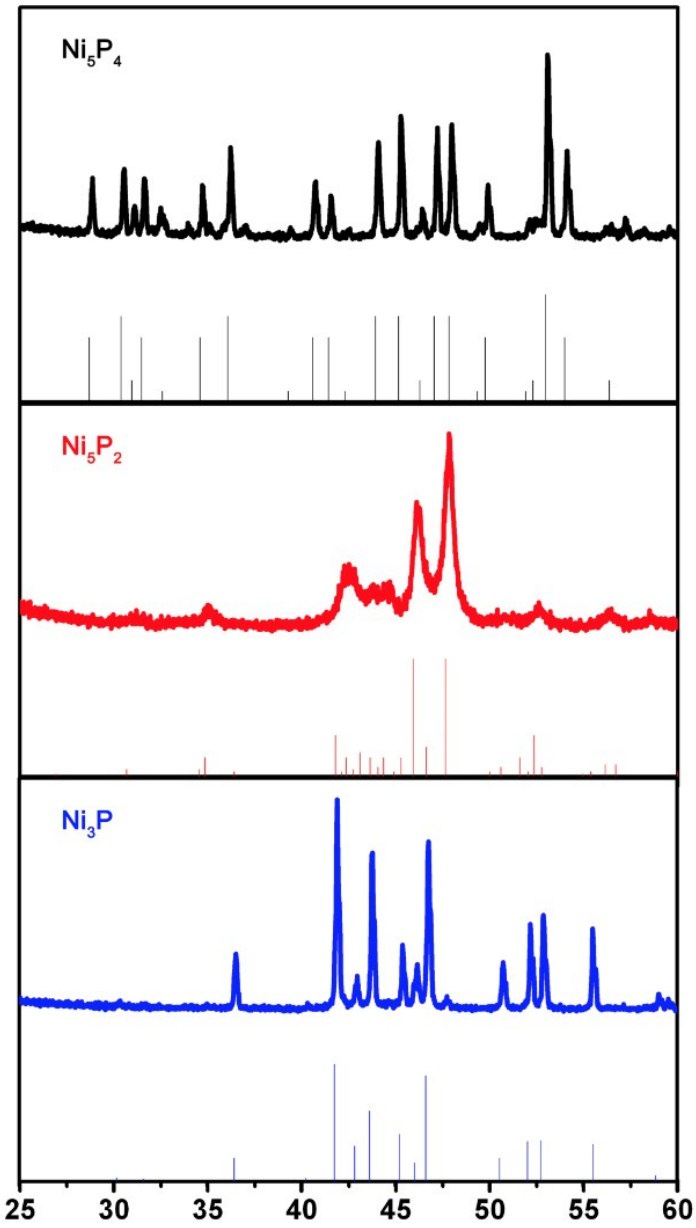

Figure S4. The powder X-ray diffraction pattern for Ni_5P_4 (black color), Ni_5P_2 (red color), Ni_3P (blue color).

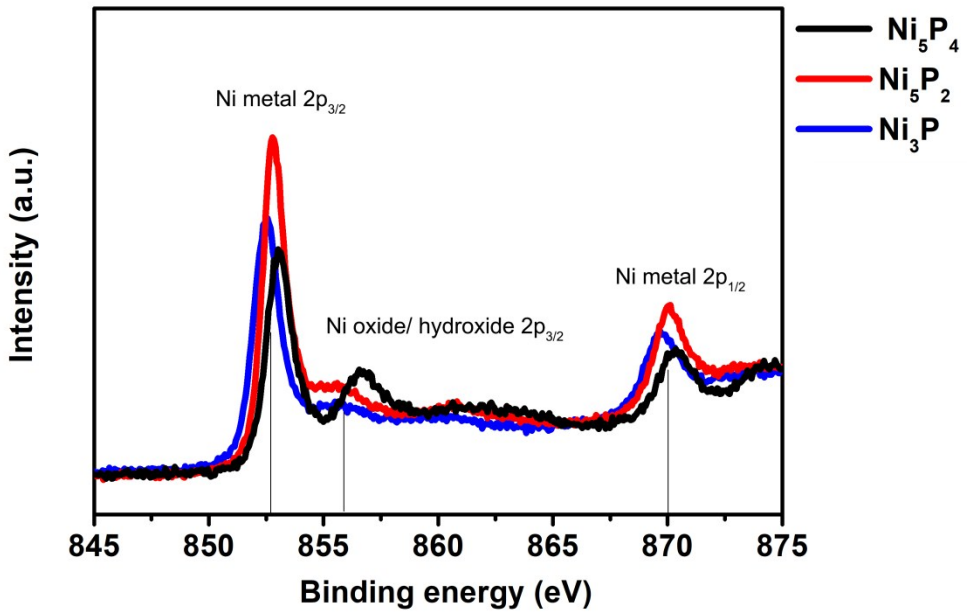

Figure S5. Ni 2p X-ray photoelectron spectrum of Ni_5P_4, Ni_5P_2 and Ni_3P before OER.

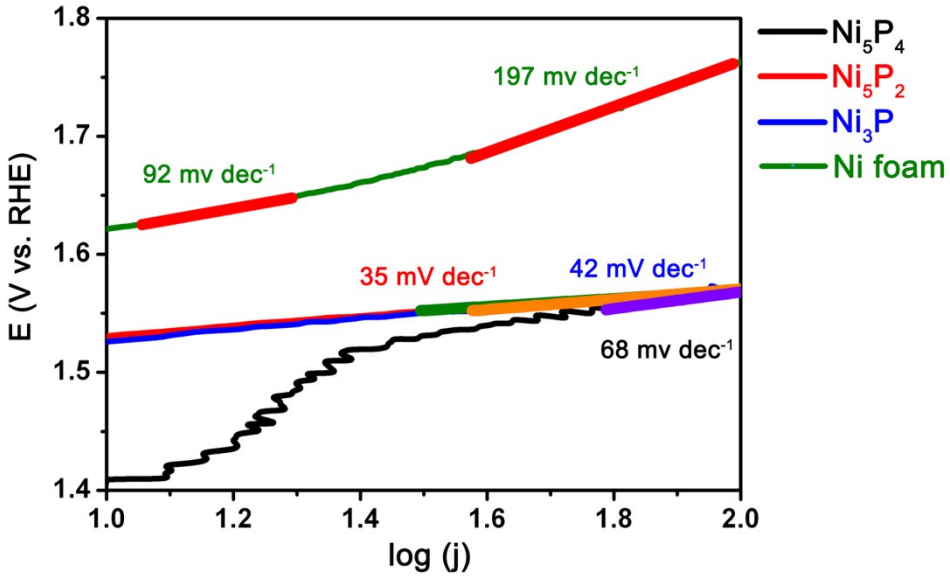

Figure S6. Tafel slopes of Ni_5P_4 (black color), Ni_5P_2 (red color), Ni_3P (blue color) and nickel foam (green color).

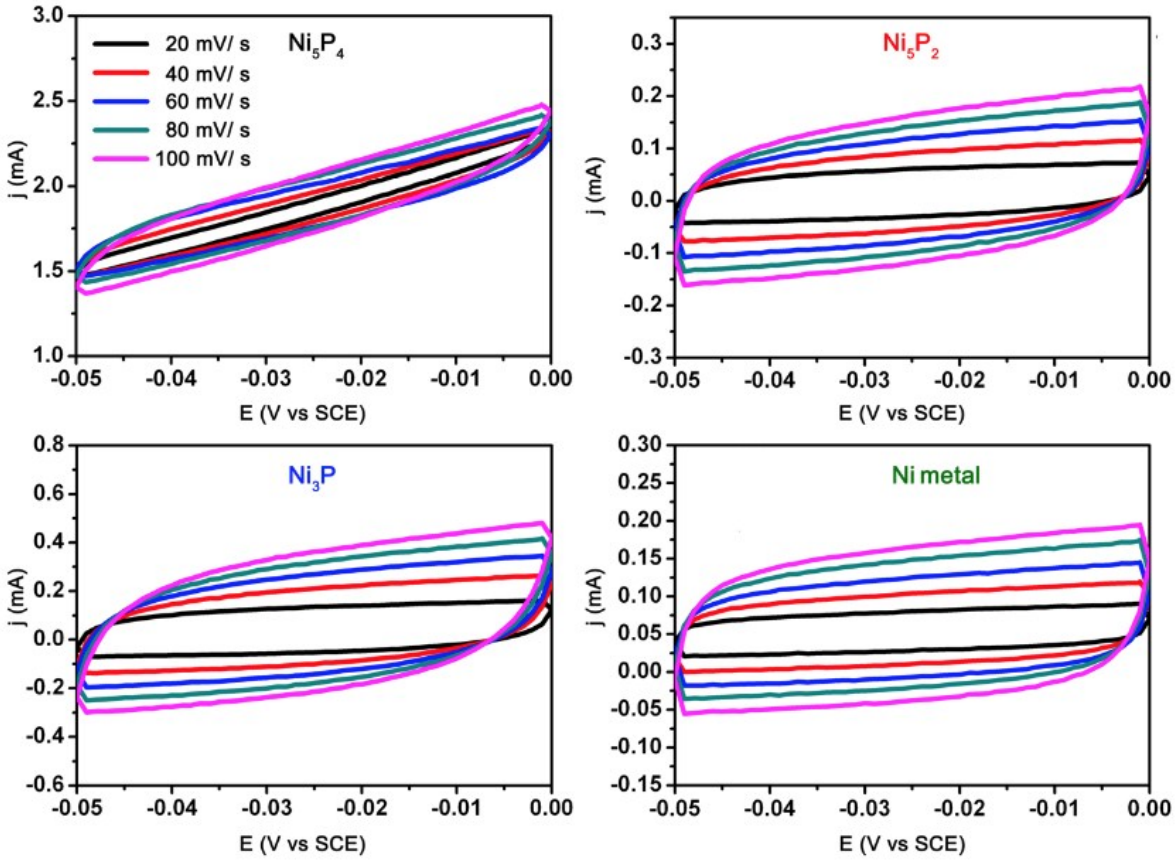

Figure S7. Cyclic voltammograms of Ni_5P_4 (black color), Ni_5P_2 (red color), Ni_3P (blue color) and Ni foam (green color) at 1.0 M KOH.

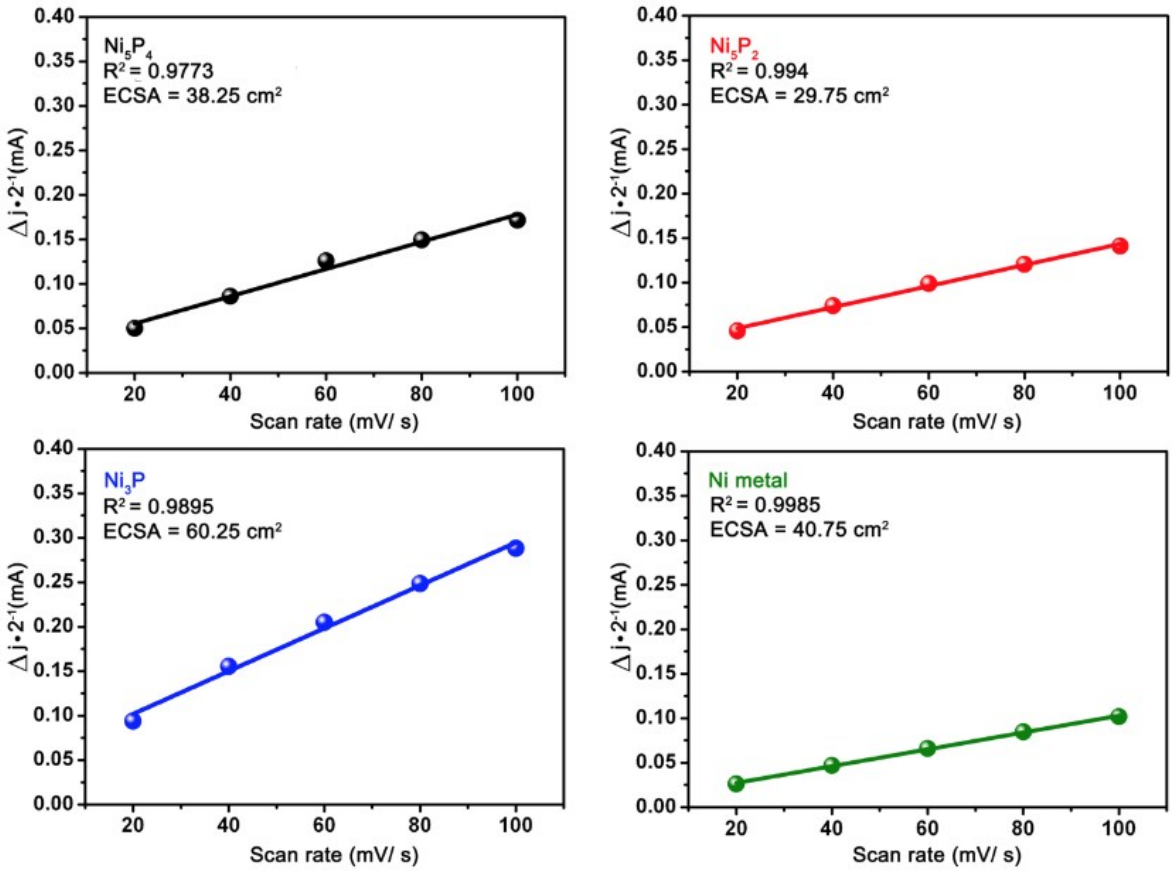

Figure S8. Capacitive current density as a function of scan rate (20 – 100 mV/ s). The derived electrochemically active surface area (ECSA) of each compound from the linear regression slope (specific capacitance 40 μF/ cm^2) is also included.

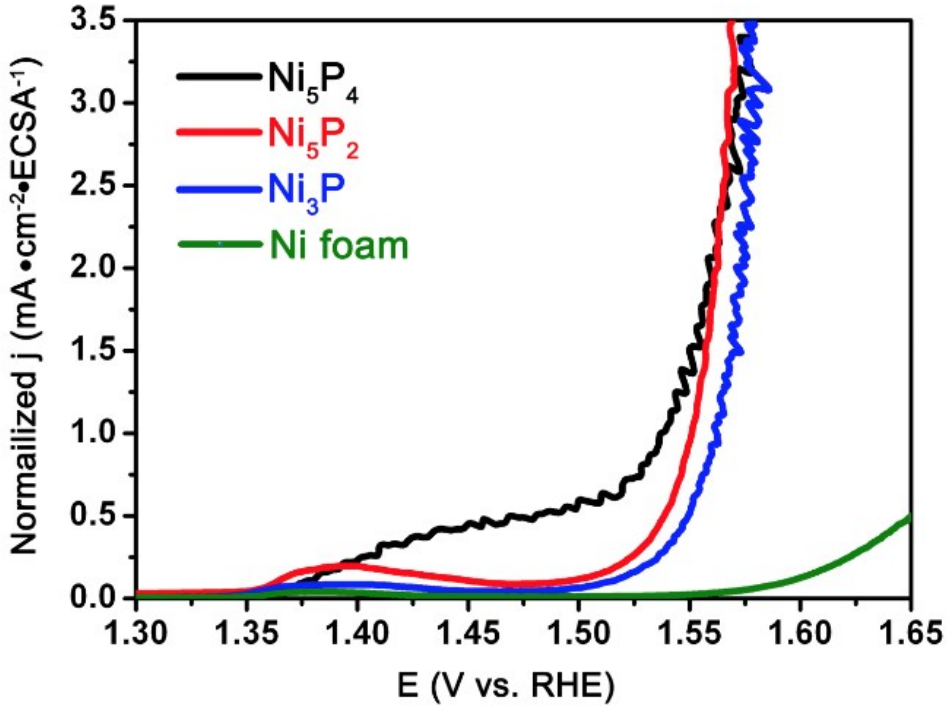

Figure S9. Normalized linear sweep voltammograms (based on ECSA) for the OER of Ni_5P_4 (black color), Ni_5P_2 (red color), Ni_3P (blue color) and Ni foam (green color) at 1.0 M KOH (scan rate: 1 mV/s).

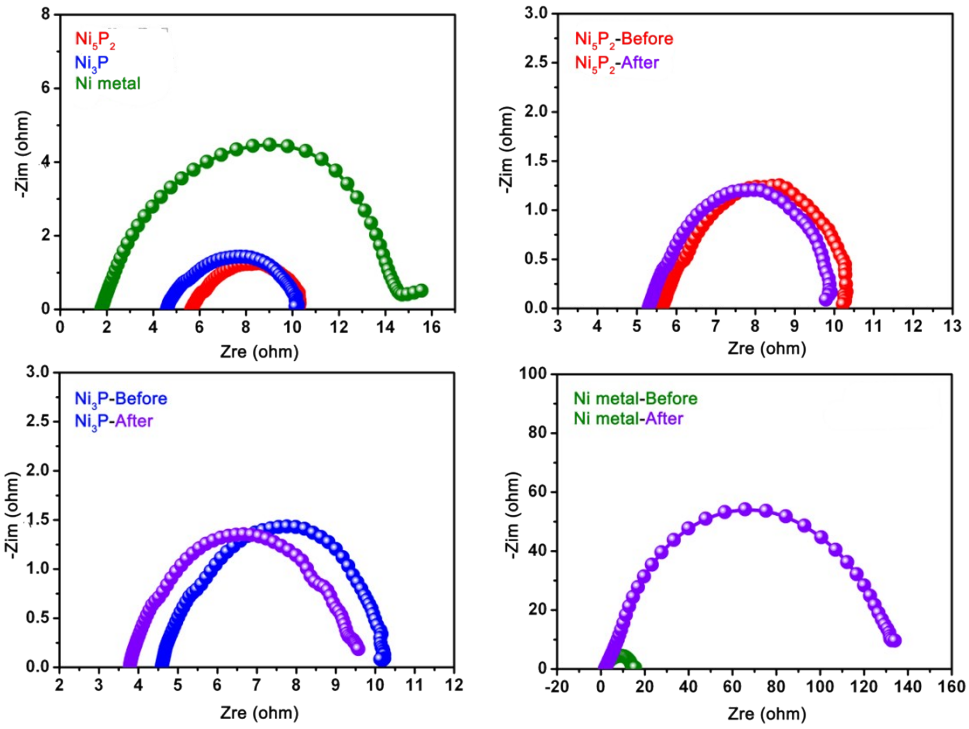

Figure S10. Electrochemical impedance spectroscopy (EIS) analysis of Ni_5P_2 (red color), Ni_3P (blue color) and Ni foam (green color) in 1.0 M KOH. The Nyquist plot for each sample after chronoamperometry test was also included and colored in purple.

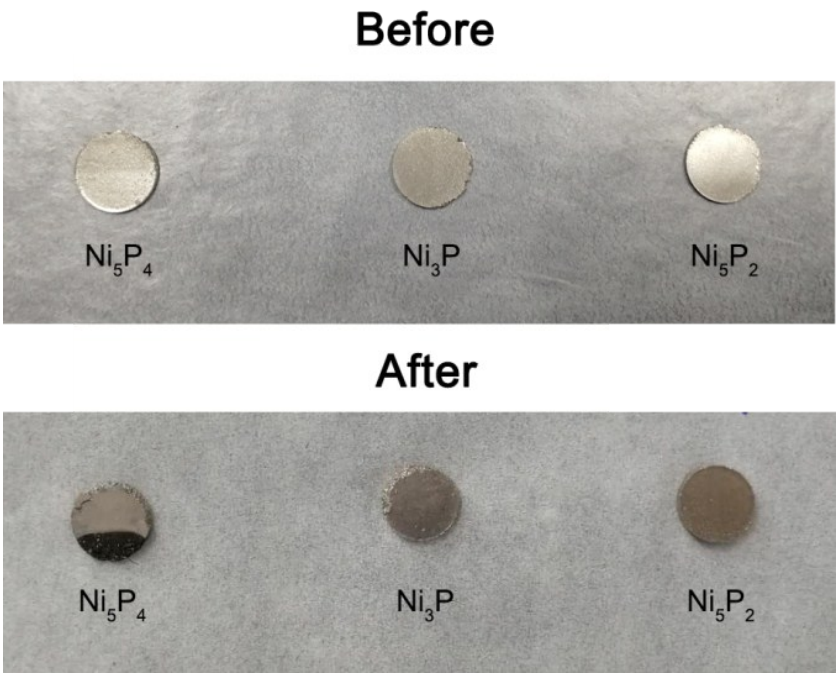

Figure S11. Photos of all samples before and after OER test.

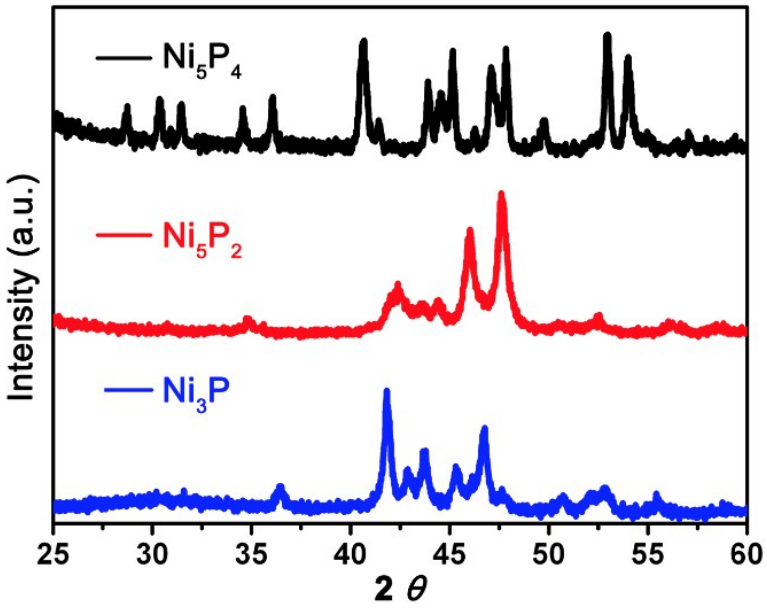

Figure S12. The powder X-ray diffraction pattern for Ni_5P_4 (black color), Ni_5P_2 (red color), Ni_3P (blue color) after chronoamperometry test.

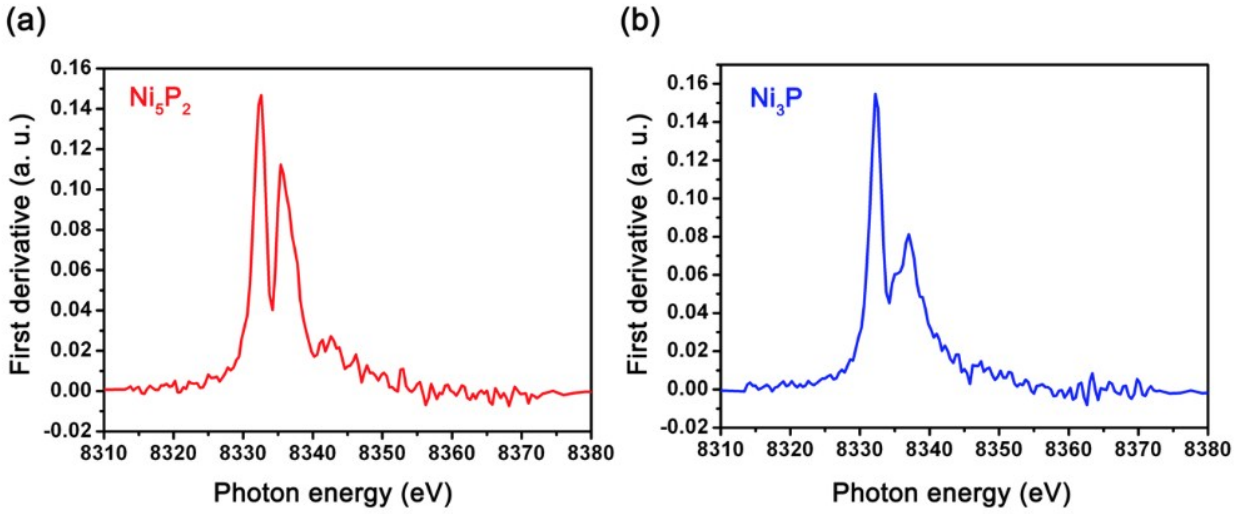

Figure S13. First derivate of X-ray adsorption near-edge structure (XANES) of Ni K-edge for (a) Ni_5P_2 and (b) Ni_3P.

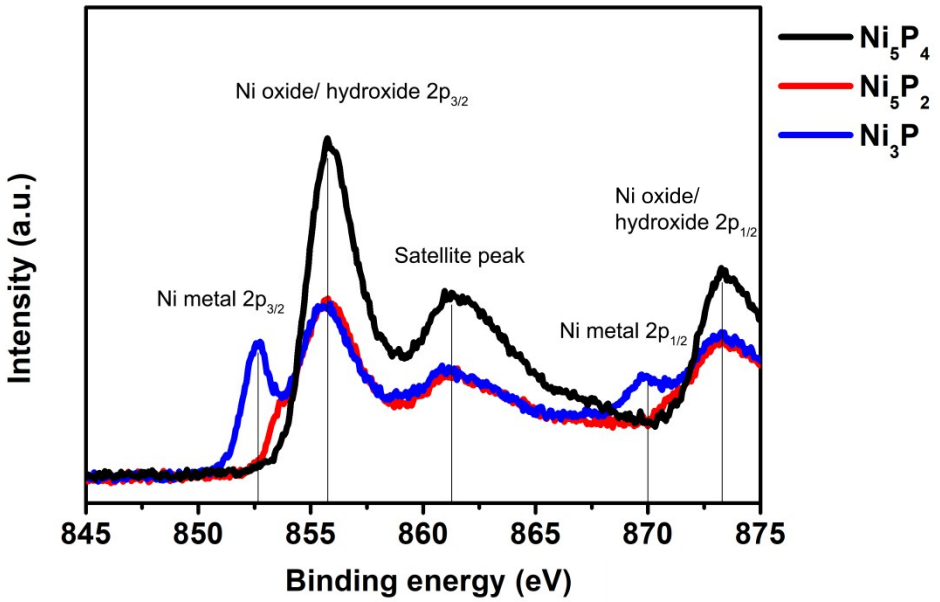

Figure S14. Ni 2p X-ray photoelectron spectrum of Ni_5P_4, Ni_5P_2 and Ni_3P after OER.

Table S1. The Atomic Ratio of Ni_5P_4, Ni_5P_2 and Ni_3P before and after chronoamperometry test.

	Element	Atomic ratio (%)	
		Before	After
Ni_5P_4	Ni	54.49	32.7
	P	45.51	13.27
	O	*	54.03
	Ni/P	1.20	2.46
Ni_5P_2	Ni	69.01	69.72
	P	30.99	30.28
	Ni/P	2.23	2.30
Ni_3P	Ni	73.4	72.55
	P	26.6	27.45
	Ni/P	2.76	2.64

Table S2. Overpotential (mV) and Tafel slope (mV•decade^{-1}) of Oxygen evolution (OER) under Alkaline Conditions.

	OER		
	Overpotential (mV)		Tafel (mV•decade^{-1})
	10 mA•cm^{-2}	100 mA•cm^{-2}	
Ni_5P_4	*		68
Ni_5P_2	300	340	35
Ni_3P	296		42

Table S3. Applied overpotential of chronoamperometry test

Sample	OER overpotential (RHE)
Ni_5P_4	*
Ni_5P_2	368 / 432
Ni_3P	367.5 / 396